# The Influence of Hybrid Coatings on Scaling-Resistant Properties of X33CrNiMn23-8 Steel

K.Adamaszek[1], Z.Jurasz[1], L. Swadzba[2], Z.Grzesik[3]*, S.Mrowec[3]

[1]*BOSMAL Automotive Research and Development Center, ul. Sarni Stok 93, 43-300 Bielsko-Biala, Poland*
[2]*The Silesian University of Technology, Faculty of Materials Science and Metallurgy, ul. Krasinskiego 8, 40-019 Katowice, Poland*
[3]*University of Science and Technology, Faculty of Materials Science and Ceramics, al. A. Mickiewicza 30, 30–059 Krakow, Poland*

(Received January 10, 2007: final form January 24, 2007)

## ABSTRACT

The influence of two-layer hybrid coatings on the oxidation behavior of X33CrNiMn23-8 steel, utilized in valves of Diesel engines, have been studied as a function of temperature (873 – 1273 K) and oxygen pressure ($1–10^5$ Pa), using modern microthermo-gravimetric techniques. Phase composition of the oxidation products (scale) was investigated by X-ray diffraction (XRD), and the morphology and chemical composition of reaction products by electron probe micro analysis (EPMA) and scanning electron microscopy (SEM) with energy disperse X-ray analyzer (EDX). It has been found that uncoated material shows very good oxidation resistance under isothermal conditions, comparable with that of chromia formers, due to the formation on its surface of $Cr_2O_3$ scale. However, beneath the scale, steel undergoes rapid degradation, as a result of crack formation; the deeper the penetration, the longer is the oxidation time. On the other hand, no cracks were observed in the coated steel and the oxidation rate was even slightly lower than that of uncoated material.

**Keywords:** steel, oxidation kinetics, hybrid coatings.

## 1. INTRODUCTION

One of the most frequently utilized materials for the production of valves in Diesel engines is X33CrNiMn23-8 steel, containing a rather high concentration of chromium and nickel. This material is working under very severe conditions, because of relatively high temperature (~ 1173 K) and very aggressive properties of combustion gases. In addition to oxygen, these gases contain carbon oxides and water vapor, nitrogen oxides and sulphur traces. The mechanism of corrosion of valve materials under such conditions is very complex and still not satisfactorily understood /1/. One of the possible methods to protect the valve surface against corrosion attack of combustion gases may consist in utilizing ceramic coatings /2/. However, the application of suitable coatings first needs detailed information on the kinetics and mechanism of corrosion of pure and coated valve material as a function of temperature and gas composition.

Thus, the present paper is an attempt to summarize the results obtained in oxygen atmosphere; the influence of water vapor as well as that of carbon and nitrogen oxides will be described in a subsequent paper.

* Corresponding author.
e-mail: grzesik@uci.agh.edu.pl
Fax number: +48 12-6172493

## 2. MATERIALS AND EXPERIMENTAL PROCEDURE

**Table 1**
The chemical composition of X33CrNiMn23-8 steel

| Chemical composition, at. % | | | | | | | | | |
|---|---|---|---|---|---|---|---|---|---|
| C | Mn | Si | Cr | Ni | N | P | S | Mo | W |
| 0.35 | 3.3 | 0.63 | 23.4 | 7.8 | 0.28 | 0.014 | <0.005 | 0.11 | 0.02 |

The steel with the composition given in Table 1 was used as a starting material. The technology of preparation of this material was rather complex and consisted of plastic hot working and subsequent suitable heat treatment. The rods with a diameter of about 20 mm were cut into flat discs with the thickness of 1 mm and the surface of some of these samples, destined for oxidation without coating, were polished with emery papers and diamond pastes to obtain mirror-like surfaces. The rest of the specimens were covered with a hybrid coating with a thickness of about 0.3 mm. This coating was composed of two layers, the inner one built of Ni22Cr10AlY alloy and the outer ceramic layer of $ZrO_2 \cdot Y_2O_3$. This hybrid coating has been obtained by plasma spraying. The inner NiCrAlY layer of the coating ensures high oxidation resistance and the outer ceramic layer plays the role of thermal barrier coating.

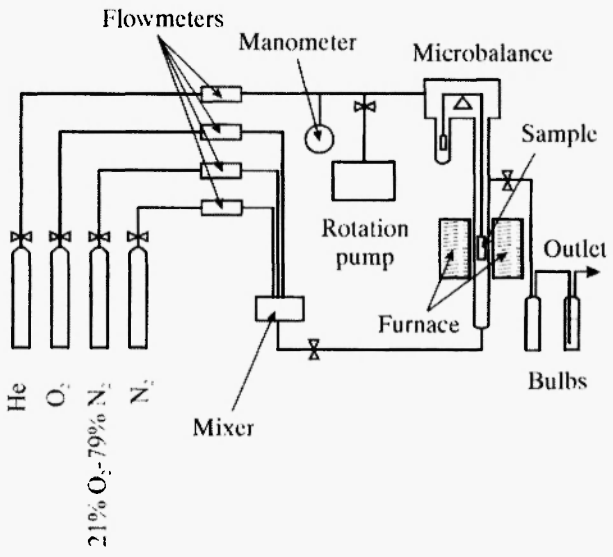


**Fig. 1:** The scheme of microthermogravimetric apparatus for studying the kinetics of metal oxidation.

The oxidation kinetics of both types of specimens (uncoated and coated ones) have been studied thermogravimetrically, as a function of temperature (873 – 1273 K) and oxygen pressure (1 – $10^5$ Pa), in the apparatus shown schematically in Fig. 1. The partial pressure of oxygen in the $O_2 - N_2$ gas mixture, flowing through the reaction chamber with the rate of 50 ml/min, has been obtained by suitable composition of this atmosphere of the total pressure of $10^5$ Pa. The second gas stream of pure helium was flowing through the microbalance chamber to protect electronic microbalance against oxygen attack. A detailed description of this novel microthermogravimetric equipment is described elsewhere /3/.

Phase composition of the oxidation products (scale) has been studied by X-ray diffraction (XRD), and the morphology and chemical composition of reaction products by electron probe micro analysis (EPMA) and scanning electron microscopy (SEM) with energy disperse X-ray analyzer (EDX).

The experimental procedure in studying the oxidation kinetics was as follows. The metal sample was suspended on the electronic microthermobalance in the reaction chamber and the flow of $O_2$-$N_2$ gas mixture of suitable composition was started. Simultaneously, the reaction furnace, moved down below the reaction zone, was heated to the temperature, at which the sample was oxidized. When the desired temperature in the furnace was established, it was raised to reaction position (see Fig. 1) and weight gains of the sample were continuously registered as a function of time, with the accuracy of the order of $10^{-6}$ g. This procedure was repeated several times at different temperatures and partial pressures of oxygen in order to determine the dependence of the oxidation rate on these two parameters. The details of the microthermogravimetric apparatus, utilized in this study and that of experimental procedure are described elsewhere /3, 4/.

## 3. RESULTS AND DISCUSSIONS

The results of oxidation rate measurements of uncovered specimens are shown in Figs. 2 and 3, in linear plot. As can be seen, the oxidation rate decreases continuously with increasing time and is temperature

dependent (Fig. 2), but does not virtually depend on oxygen pressure (Fig. 3). These results are shown once again in Figs. 4 and 5 in parabolic plot, clearly indicating that the process of corrosion follows strictly parabolic kinetics, being thus diffusion controlled. Temperature and pressure dependence of the parabolic rate constant calculated from these results are shown in Arrhenius (Fig. 6) and doubly logarithmic (Fig. 7) plots, respectively.

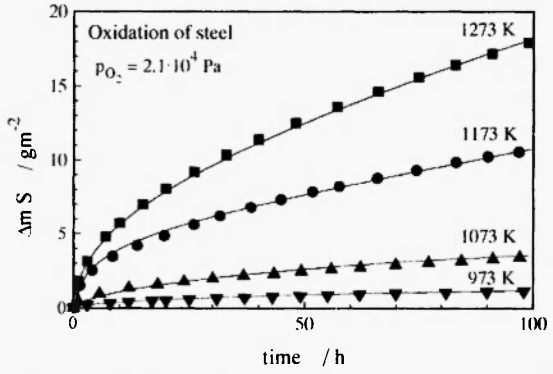


**Fig. 2:** Oxidation kinetics of uncoated steel at several temperatures (linear plot).

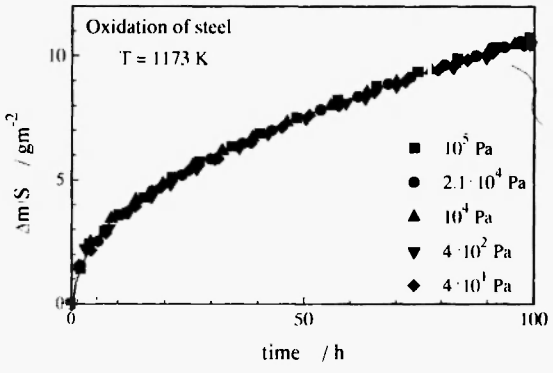


**Fig. 3:** Oxidation kinetics of uncoated steel at several oxygen pressures (linear plot).

From X-ray diffraction patterns, presented in Fig. 8, it follows that the scale is heterogeneous and built of chromium oxide, $Cr_2O_3$, and magnetite $Fe_3O_4$. EPMA analysis has shown, in turn, that chromium oxide forms compact inner layer of the scale and the thin outer layer is composed of $Fe_3O_4$ doped with chromium and manganese.

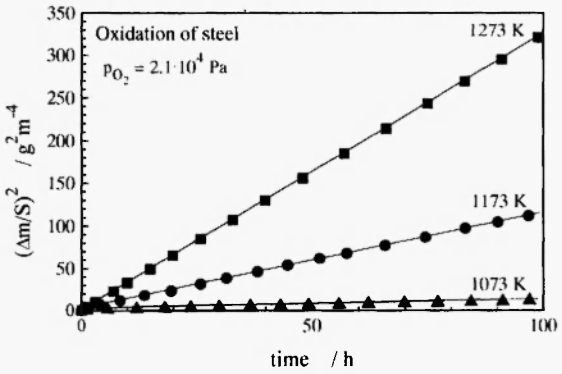


**Fig. 4:** Oxidation kinetics of uncoated steel at several temperatures (parabolic plot).

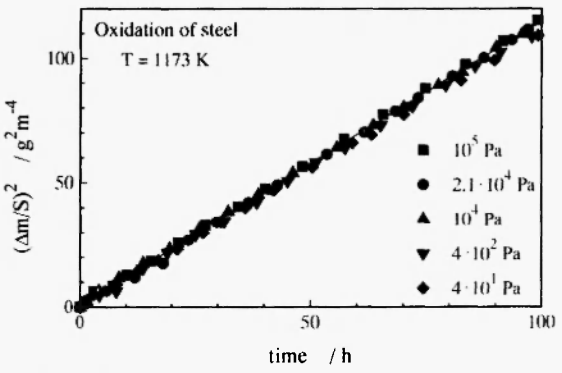


**Fig. 5:** Oxidation kinetics of uncoated steel at several oxygen pressures (parabolic plot).

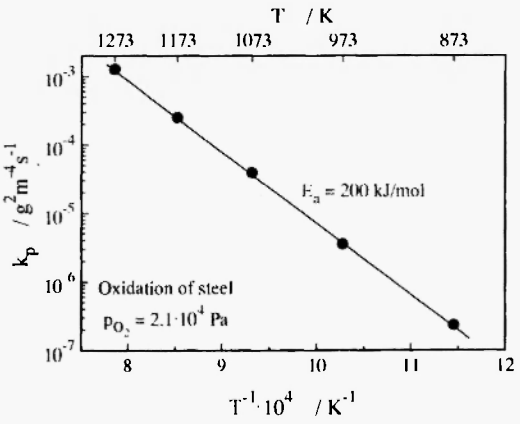


**Fig. 6:** Temperature dependence of the oxidation rate of uncoated steel (Arrhenius plot).

From phase composition of the scale, it follows that the inner compact $Cr_2O_3$ scale constitutes the barrier layer for the outward diffusion of chromium /5, 6/ and consequently, the studied material shows very good

corrosion resistance in oxidizing atmospheres. From the comparison of these kinetic results with those of model chromia formers /5, 6/, presented in Fig. 9, it follows clearly that the oxidation rate of our material is, in the studied temperature range, virtually the same as that of model binary alloys, on the surface of which a homogeneous, protective $Cr_2O_3$ scale is formed. It may then be concluded that the studied valve material shows excellent resistance to oxygen attack under isothermal conditions. However, SEM images of metallographic cross-sections of specimens oxidized at several temperatures (Figs. 10 and 11) indicate that beneath the scale, the steel undergoes dramatic degradation, as a result of crack formation; the deeper the penetration, the longer is the oxidation time. These results explain the restricted life time of valves in Diesel engines, in spite of very good protective properties of scale and this is one of the main reasons why the possible role of protective coatings must be investigated.

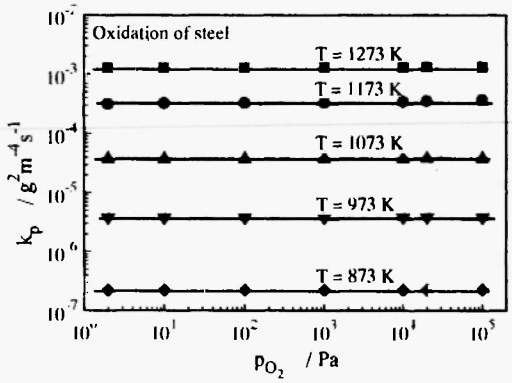


**Fig. 7:** Pressure dependence of the oxidation rate of uncoated steel for several temperatures (double logarithmic plot).

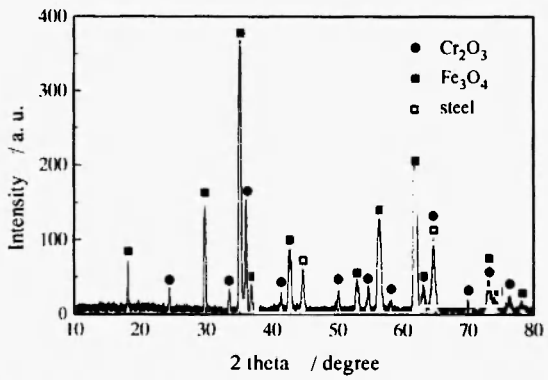


**Fig. 8:** X-ray diffraction pattern for uncoated steel, oxidized at 1173 K for 100 hours.

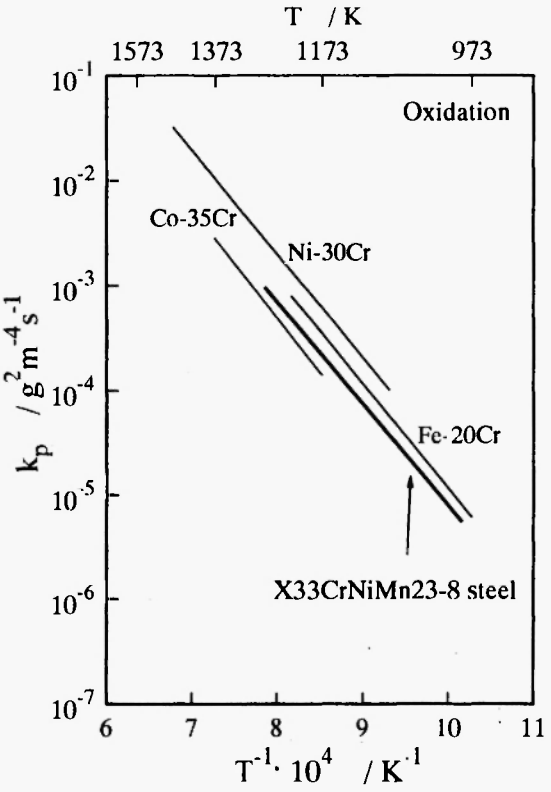


**Fig. 9:** Temperature dependence of the oxidation rate of uncoated steel on the background of analogous dependence for several chromia formers.

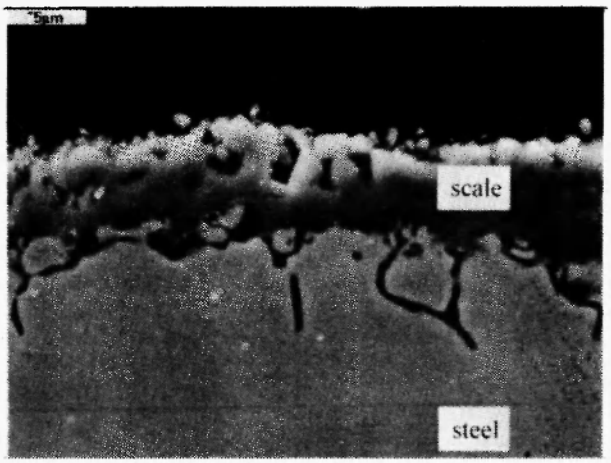


**Fig. 10:** SEM image of the cross-section of steel sample, oxidized at 1173 K during 100 hours.

Oxidation kinetics of coated specimens have been studied under the same experimental conditions, as a function of temperature and oxygen pressure. The results obtained in different temperatures (Fig. 12) and

oxygen pressures (Fig. 13) have shown different behavior from that observed in the case of uncoated samples. From these figures it follows, namely, that the oxidation process in early stages of the reaction proceeds much faster and in later stages decreases more rapidly, than in the case of uncoated specimens. Consequently, in the first stage of the reaction, the process does not follow parabolic kinetics and only in the second stage, after 60-70 hours, parabolic course of the reaction is observed (Fig. 14). The comparison of the oxidation kinetics of both types of specimens, presented in Fig. 15 suggests that in later stages the rate of corrosion of coated material is very similar to that observed in the case of uncoated samples; however, the results presented in Arrhenius plot in Fig. 16 clearly indicate that the oxidation rate of coated specimens is about half an order of magnitude lower than that of uncoated steel.

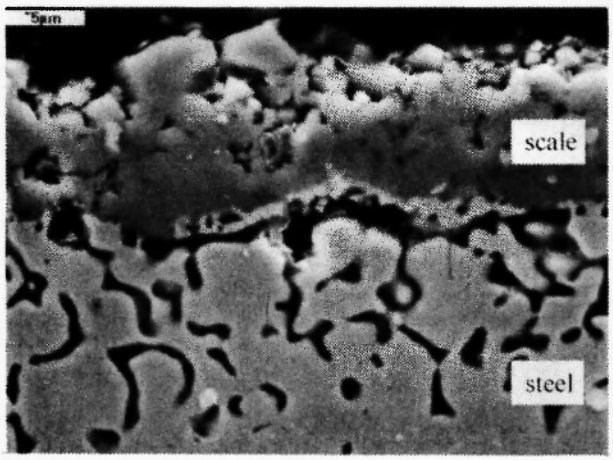


**Fig. 11:** SEM image of the cross-section of steel sample, oxidized at 1173 K during 200 hours.

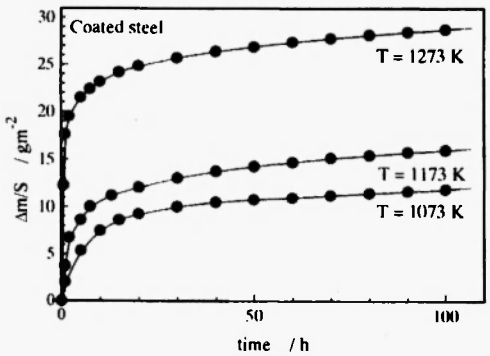


**Fig. 12:** Oxidation kinetics of coated steel at several temperatures (linear plot).

The question then arises, what are the reasons why the oxidation rate of coated specimens does not follow parabolic rate law in the early stages of the reaction and secondly, why the oxidation rate of coated samples under steady state conditions is considerably lower than that of uncoated material. The explanation of both these problems is rather difficult, because of complex chemical composition of scales and coatings. One may speculate, however, that, due to the quite highly developed surface of the coating (Fig. 17), in the early stages of the reaction a much higher oxidation rate, calculated from mass gains (Δm) of the oxidized sample, divided by its geometrical area (S) does not reflect the real oxidation rate. With the reaction progress, surface roughness continuously decreases and after 60-70 hours mass gains of the sample divided by geometrical surface area, correctly illustrate the oxidation run (Figs. 18 and 19) and parabolic course of the reaction is observed.

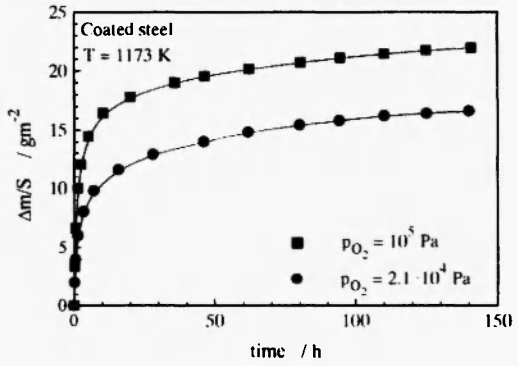


**Fig. 13:** Oxidation kinetics of coated steel at two different oxygen pressures (linear plot).

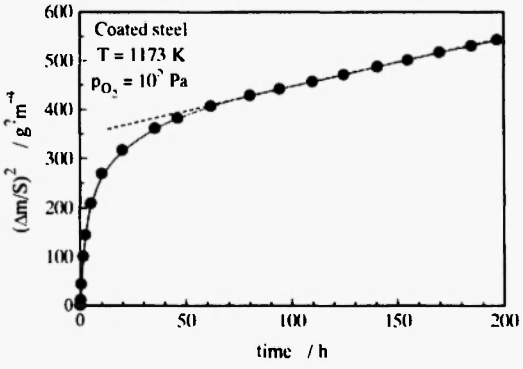


**Fig. 14:** Oxidation kinetics of coated steel for T = 1173 K and $p_{O_2} = 10^5$ Pa (parabolic plot).

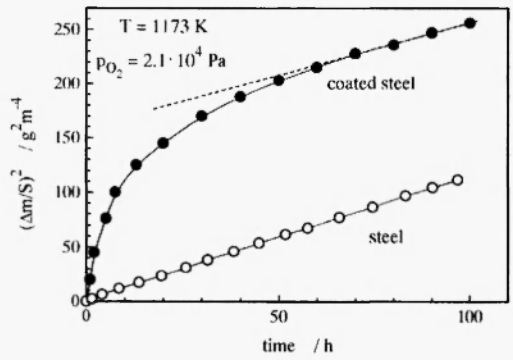


**Fig. 15:** Comparison of the oxidation kinetics of coated and uncoated steel for T = 1173 K and $p_{O_2} = 2.1 \cdot 10^4$ Pa (parabolic plot).

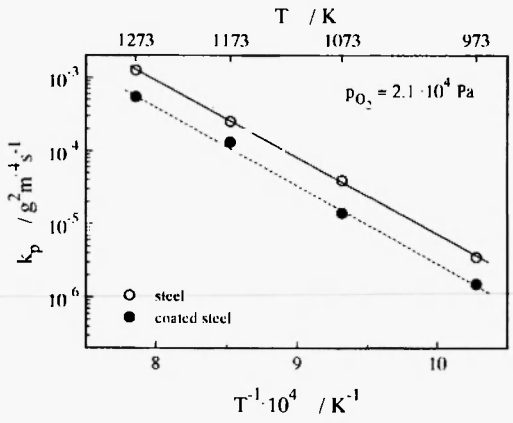


**Fig. 16:** Temperature dependence of the oxidation rate of coated and uncoated steel (Arrhenius plot).

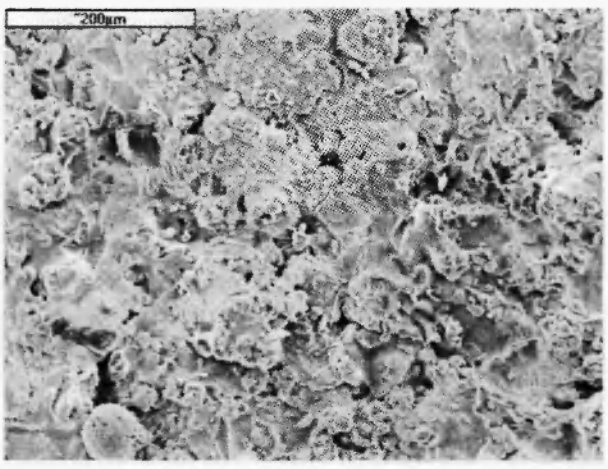


**Fig. 17:** SEM image of the surface of coated steel sample.

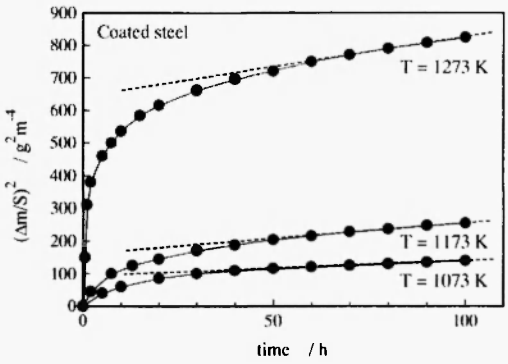


**Fig. 18:** Oxidation kinetics of coated steel at several temperatures (parabolic plot).

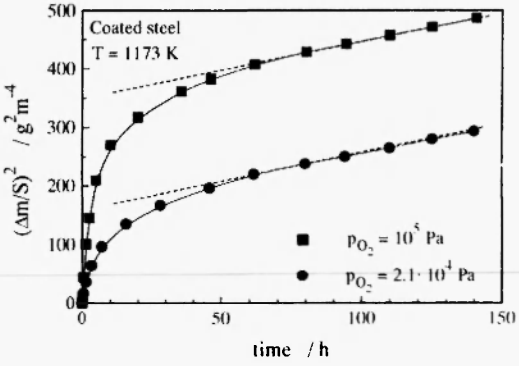


**Fig. 19:** Oxidation kinetics of coated steel under two different oxygen pressures at 1173 K (parabolic plot).

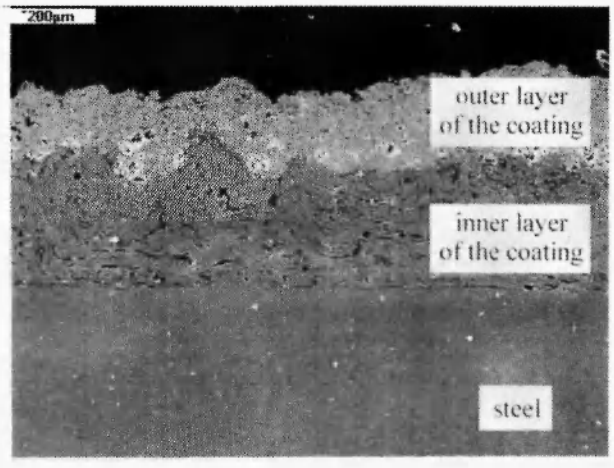


**Fig. 20:** SEM image of the cross-section of coated steel sample, oxidized at 1173 K during 200 hours.

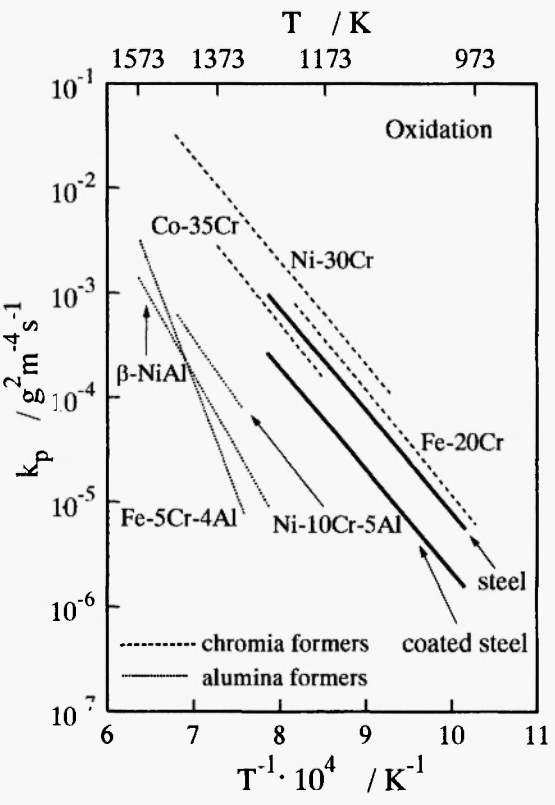


**Fig. 21:** Temperature dependence of the oxidation rate of the coated steel on the background of analogous dependence for several chromia and alumina formers.

As far as the lower oxidation rate of coated specimens is concerned, this phenomenon may be related to a rather high concentration of aluminum in coated material. It is well known that alumina scale ($\alpha$-$Al_2O_3$) shows excellent, even better than chromia ($Cr_2O_3$) protective properties and consequently modern oxidation resistant alloys, containing aluminum and called alumina formers, show even better corrosion resistance than chromia formers /6, 7/. X-ray and SEM analysis have shown that the phase and chemical composition of coatings is very complex and it is very difficult to formulate same definite conclusions concerning oxidation products within the coating. Nevertheless, qualitative analysis has shown that in the interior of the coating, as shown in Fig. 20, alumina scale has been found at the surface of the inner NiCrAlY layer. This barrier layer is, then, more protective than pure chromia scale and consequently, the oxidation rate of coated samples is, in fact, higher than that of pure alumina formers, but lower than chromia formers, as illustrated by a collective plot, presented in Fig. 21.

However, very good oxidation resistance of coated specimens does not constitute the main advantage of coatings. A much more important positive influence of coating consists in the dramatic reduction of crack formation in the interior of coated material. This conclusion follows directly from the microphotograph, presented already in Fig. 20. It follows from this figure that, after prolonged oxidation time, no cracks are observed beneath the coatings in contrast to uncoated material (Figs. 10 and 11).

## 4. CONCLUSIONS

The results described in the presented paper allow the following conclusions to be formulated.

X33CrNiMn23-8 steel, utilized for the production of valves in Diesel engines, shows very good oxidation resistance under isothermal conditions, comparable with that of chromia formers, due to the formation on its surface protective $Cr_2O_3$ scale. However, beneath the scale, steel undergoes dramatic degradation as a result of cracks formation, penetrating the deeper, the longer is the oxidation time and this is a main reason, why the valves shows rather restricted life time.

On the other hand, no cracks are observed in the same valve material with two-layer hybrid coating, and the oxidation rate is even slightly lower than that of uncovered steel. The lower oxidation rate of coated material may be tentatively explained by the formation in the interior of coating of alumina layer.

## REFERENCES

1. D. Naumienko, L. Singheiser and W.J. Quadakkers, "Oxidation Limited of FeCrAl Based Alloys During Thermal Cyclic", in: *Proceedings of an EFC Workshop,* held in Frankfurt/Main, edited by M. Schutze and W.J. Quadakkers, 1999; p. 287-306.
2. M. Beukenberg, "Thermal Fatigue Evaluation of EB-PVD TBCs with Different Bond Coats", in

*Proceedings of Turbine Forum* (2006), *Advances Coatings for High Temperatures*, held in Nice, April 26-28, 2006.

3. S. Mrowec and Z. Grzesik, *J. Phys. Chem. Solids*, **65**, 1651 (2004).
4. S. Mrowec, Z. Grzesik and B. Rajchel, *High Temp. Materials and Processes*, **23**, 59 (2004).
5. P. Kofstad, *High Temperature Corrosion*, Elsevier Applied Science, London and New York, 1988; p. 389.
6. S. Mrowec, *High Temp. Materials and Processes*, **22,** 1 (2003).
7. P. Kofstad, *High Temperature Corrosion*, Elsevier Applied Science, London and New York, 1988; p. 408.